

# Using Hilbert Curves to Organize, Sample, and Sonify Solar Data

## Abstract

How many ways can we explore the Sun? We have images in many wavelengths and squiggly lines of many parameters that we can use to characterize the Sun. We know that while the Sun is blindingly bright to the naked eye it also has regions that are dark in some wavelengths of light and bright in others. All of those classifications are based on vision. Hearing is another sense that can be used to explore solar data. Some data, such as the sunspot number or the extreme ultraviolet spectral irradiance, can be readily sonified by converting the data values to musical pitches. Images are more difficult. Using a raster scan algorithm to convert a full-disk image of the Sun to a stream of pixel values is dominated by the pattern of moving on and off the limb of the Sun. A sonification of such a raster scan will contain discontinuities at the limbs that mask the information contained in the image. As an alternative, Hilbert curves are continuous space-filling curves that map a linear variable onto the two-dimensional coordinates of an image. We have investigated using Hilbert curves as a way to sample and analyze solar images. Reading the image along a Hilbert curve keeps most neighborhoods close together as the resolution (i.e., the order of the Hilbert curve) increases. It also removes most of the detector size periodicities and may reveal larger-scale features. We present several examples of sonified solar data, including the sunspot number, a selection of extreme ultraviolet (EUV) spectral irradiances, different ways to sonify an EUV image, and a series of EUV images during a filament eruption.

## 19 I. INTRODUCTION

20 Sonifying a data set has the basic purposes of making data accessible to the blind and allowing  
21 the data to serve as an adjunct to other senses. It can also help all to appreciate or understand a  
22 data set in a new way. Although a one-dimensional data set can be sonified by scaling the data  
23 to pitches, image data is a more ambitious target. The data has variations in two dimensions that  
24 should be represented by the sonification, and variations seen in a series of images are even more  
25 difficult to sonify. Solar data is often in the form of images and the changes in time and space are  
26 an integral part of understanding solar variations. We will describe sonifying several solar datasets,  
27 including an exploration of ways to sonify solar images in space and time.

28 Composers have used many ways to create sounds and music that mimic the natural and me-  
29 chanical worlds. Camille Saint-Saëns used pianos and other instruments to imitate about 14 an-  
30 imals in *The Carnival of the Animals*.<sup>1</sup> Old-time fiddle tunes use the flexibility of the combined  
31 performer and violin to imitate chickens and other natural sounds. Luigi Russolo built “intonaru-  
32 mori” to produce a broad spectrum of modulated, rhythmic sounds that imitated machines.<sup>2</sup> He  
33 also developed a graphical form of musical score to compose pieces for these devices. Others  
34 have produced music from time sequences of the natural world. A well-known example is Concret  
35 PH,<sup>3</sup> which was created by splicing together short, random segments of tape recordings of burning  
36 charcoal.

37 Analog electronic synthesizers provided another path. In their early stages they were often  
38 used to produce sound effects. As analog synthesizers became more capable, such as the Moog  
39 modular synthesizer,<sup>4</sup> some used them to reproduce well-known musical pieces in electronic form  
40 (e.g., *Switched-On Bach* by Wendy Carlos, 1968) while others invented new types of music (the  
41 improvisations of Keith Emerson in the works of Emerson, Lake, and Palmer.)

42 Few, if any, of these techniques are examples of sonifying data. Sonification can be as simple  
43 as the shrieking of a smoke alarm or as complicated as converting multi-dimensional data to an  
44 audible signal. The incessant beeps and whistles of electronic vital sign monitors in hospitals are  
45 one example where the change in a sound signals a change in the health of a patient. These use  
46 the 1-D structure of sound to convey information that conditions are both normal and alarming.  
47 Whistlers are an example of how scientists sonified radio frequency data to study the ionosphere.<sup>5</sup>

48 The radio signals from the interactions of lightning with the electrons in the magnetosphere are  
49 heard as descending tones lasting a few seconds at audio frequencies between 1–30 kHz.

50 **The many types and enormous quantity of solar data make it perfect for experiments in**  
51 **sonification. There are natural timescales of variation from seconds to 100's of years and ob-**  
52 **served parameters can change by several orders of magnitudes during events such as a large**  
53 **solar flare. Such variations can make sonification challenging but rewarding. One example**  
54 **is from helioseismology, the study of sound waves propagating as resonant modes inside of**  
55 **Sun. Amplitude variations of the resonant acoustic waves were audified by multiplying their**  
56 **measured frequency of several mHz (a period of roughly 5 minutes) into an audible range.**<sup>6,7</sup>  
57 **Given the success of those efforts, we decided to sonify other types of solar data with an em-**  
58 **phasis on datasets related to solar activity. Unlike the frequency shifting that was used with**  
59 **helioseismic data, synthesizer-oriented methods were developed to sonify the other solar data**  
60 **sets. We then generalized the problem to sonifying the vast archives of freely-available so-**  
61 **lar images. We also take advantage of that data's digital format that allows us to move and**  
62 **transform the data in manifold ways.**

63 Digital electronic synthesizers give us the ability to convert any type of information from a  
64 digital representation into music.<sup>8</sup> One example is that a 1-D time series can be sonified by scaling  
65 the values to musical pitches, assuming a constant duration for each value, to produce a set of  
66 Musical Instrument Digital Interface (MIDI<sup>9</sup>) commands. A MIDI-enabled synthesizer is then used  
67 to create the musical instrument waveforms and play the commands in the MIDI file. Different  
68 time series can be combined into a sonification by using different pitch ranges or timbres (the  
69 distinctive set of tones in the selected instrument) to distinguish between them. We will use the  
70 International Sunspot Number (Version 2,  $S$ ) and extreme ultraviolet (EUV) spectral irradiances  
71 from two satellites as examples of solar time series data.

72 Sonifying an image is different. Sound is intrinsically a 1-D format that evolves in time. A 2-D  
73 image must first be converted to a 1-D series of pixel values where the order of the pixels then  
74 serves as the time variable. Once the 1-D sequence exists, the pixel values are scaled to pitches,  
75 the duration is again set to a constant, and the data run through the synthesizer.

76 There are many ways to map a 2-D image (or higher-dimensional data) to a 1-D sequence. A  
77 raster scan is a linear reading of the image from the upper left to the lower right moving down to

78 the next row when the current one is read, much like reading an English language document. This  
79 can be modified into a boustrophedonic algorithm where the first row is read left to right and the  
80 next right to left, continuing in this way to the end of the image. This resembles the way an ox  
81 (Greek *bous*) plows a field and hence the term. Another way is to use a space-filling curve, such  
82 as the Hilbert used here, to map the image pixels to a sequence. We will describe using Hilbert  
83 curves to convert 2-D images into 1-D sequences and converting those sequences to sound.

84 The sonifications of these data sets will be described:

- 85 1. International Sunspot Number (annual and monthly variations)
- 86 2. Extreme ultraviolet (EUV) spectral irradiances as a time series and a spectrum
- 87 3. A complete EUV image and seven subimages
- 88 4. A montage of EUV images showing a filament liftoff

89 All of the sound files are available as .MIDI and .MP3 files at [https://sdo.gsfc.nasa.gov/sonify/](https://sdo.gsfc.nasa.gov/sonify/table.html)  
90 [table.html](https://sdo.gsfc.nasa.gov/sonify/table.html).

91 We start by introducing some useful musical concepts. That will be followed by a discussion  
92 of the synthesizer used and the analysis of of the 1-D data sets. The image data will be introduced,  
93 and an example using a raster scan to convert the data to 1-D will be described. We will then  
94 describe the Hilbert curves used to address the image data and present several ways to sonify the  
95 images. We discuss what can be learned from these sonifications and end with several conclusions  
96 on the utility of this method. All of the science datasets are open-source and are available at the  
97 locations listed in the Acknowledgements.

## 98 II. SONIFYING DATA

99 The JythonMusic software described in Manaris and Brown<sup>10</sup> was used to convert a data series  
100 into MIDI commands and drive a synthesizer. The concepts and terms we use to convert data to  
101 music are:

- 102 • Pitch: One of 128 frequencies (spanning 10.75 octaves of the 12-tone equal-tempered scale),  
103 from 8.18 Hz [ $C_{-1}$ ] – 12.54 kHz [ $G_9$ ]), with Middle C ( $C_4$ , 261.63 Hz) roughly in the

104 middle at position 60. Twenty one pitches are added below the lowest key on the piano  
 105 and 19 pitches above the highest key. A range of only 128 values is small compared to the  
 106 linear range of many solar and geophysical data sets. It is also small compared to the pitch  
 107 discrimination of human ears. Untrained humans can discern pitch changes of  $\approx 0.3\%$ ,<sup>11</sup>  
 108 so roughly 43000 pitches would be necessary to resolve that frequency range. However,  
 109 the MIDI standard only allows limited microtones at that spacing. Images encoded with the  
 110 Joint Photographic Experts Group (JPEG<sup>12</sup>) algorithm have pixel values ranging from 0–255  
 111 (either in separate channels or through a color table), so we have only half of the range in  
 112 pitches. Transforming data that varies by several orders of magnitude into logarithms can  
 113 compress the range to small enough to sonify.

- 114 • **Duration and Tempo: A beat is the natural timestep of a musical piece. The rhythmic**  
 115 **content of a piece of music is then determined by the fraction of a beat each pitch oc-**  
 116 **cupies (its duration) and the rate at which the beats are sounded (the tempo). Western**  
 117 **musical notation calls the duration “notes” and includes only a few specifications, such**  
 118 **as quarter note and whole note. Durations in a MIDI synthesizer are specified with a**  
 119 **floating point number that can vary from 0 (no time) to 1 (a quarter note) to 4 (a whole**  
 120 **note) and longer. We use durations of 0.25, corresponding to a sixteenth note, in the**  
 121 **image sonifications. Periods of time in a piece without any sound are called rests and**  
 122 **their durations are specified similar to notes. Tempo is specified by the number of beats**  
 123 **per minute (bpm); where a quarter note (QN in JythonMusic) is one beat. When the**  
 124 **tempo is increased, then the duration of each beat is decreased.**

- 125 • **Loudness:** The loudness (also called the dynamics or MIDI velocity) is set by an integer in  
 126 the range 0 (silent) to 127 (very, very loud). As the range of sound pressure level varies from  
 127 0 dB (threshold of hearing) to 120 dB (threshold of pain), the loudness maps to a change  
 128 of roughly one per dB. The response of human ears to loudness variations strongly varies  
 129 from one person to another and with frequency. The least noticeable change in loudness also  
 130 varies with frequency, but a reasonable value is 0.4 dB.<sup>13</sup> This corresponds to a 5% change  
 131 in pressure and is easily accommodated by the 128 possible values. We only use loudness to  
 132 weight the various datasets. It is also possible to encode information in the loudness, such

133 as a longer duration being louder, but we do not present such cases here.

- 134 • **Timbre:** There are 128 possible timbres in the MIDI standard, which are referred to as tracks.  
135 These timbres are not specified in the MIDI standard and a numbered timbre may sound  
136 different in different synthesizers. One track is devoted to percussion and uses the pitch  
137 designator to select a percussive timbre.
- 138 • **Pan:** Position in space is limited in this study to left-right pan. A floating point number  
139 between 0 (left) and 1 (right) determines the position, with 0.5 (centered) the default. Placing  
140 one data set in the left side and another in the right is a good way to compare two data sets.  
141 Where they agree the sounds will appear to come from the middle and otherwise they will  
142 come from separate sides.

143 JythonMusic is based on Java rather than C. Programs in JythonMusic are written in Python 2.7  
144 syntax but do not have access to many of the libraries used for numerical work. As a result, data  
145 access and extraction routines were written and executed in a C-based Python environment that  
146 provided access to the NumPy library for array manipulation. The computational sequence was to  
147 read the data, extract the appropriate part, write the extracted data to a comma-separated variable  
148 (CSV) file, read that file in the JythonMusic environment, convert the data into a MIDI file, and use  
149 the JythonMusic synthesizer to play that file. A permanent record was created by playing the MIDI  
150 commands in another synthesizer that could export the sounds to an MP3 file.

### 151 **III. SAMPLING AND SONIFYING SOLAR DATA**

152 Several types of solar data were sonified and reported here. A summary is presented in Table I,  
153 where the source, type, and name of the corresponding MP3 file are listed. The Sec. column is the  
154 part of the paper where the data is described. A version of this table, with links to the MP3 and  
155 MIDI files, is available at <https://sdo.gsfc.nasa.gov/sonify/table.html>.

#### 157 **A. International Sunspot Number**

158 The first example is the variation of the International Sunspot Number ( $S$ ) with time. The  
159 sunspot number is a weighted count of dark regions on the Sun that is often used as a long-term

TABLE I. Files for each Sonified Data Set

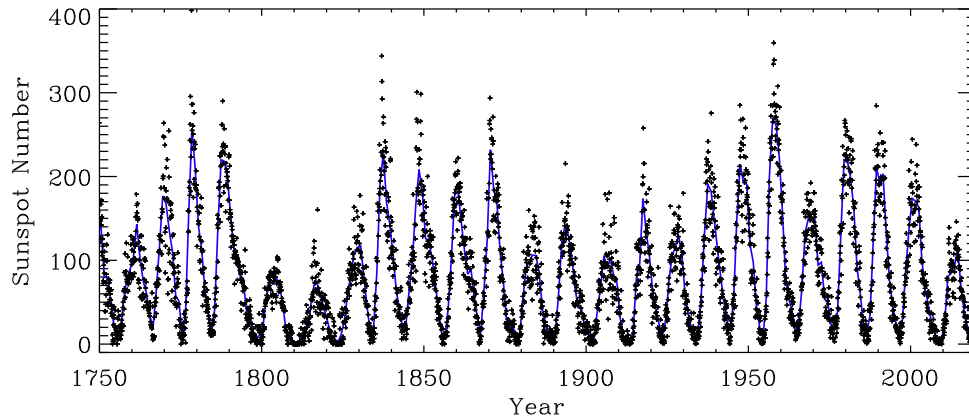
| Sec.  | Source    | Sonified Data                          | mp3 Filename                           |
|-------|-----------|--|--|
| III A | SIDC      | Sunspot number                         | TS_sunspot_annual_month.mid.mp3        |
| III B | EVE       | EUV spectral irradiances (spectrum)    | TS_EVE_sonified.mid.mp3                |
| III B | SEE       | EUV spectral irradiances (time series) | TS_SEE_sonified.mid.mp3                |
| III D | AIA 193 Å | Complete image (raster)                | AIA_193_full_image_sonified_raster.mp3 |
| V     | AIA 193 Å | Complete image (Hilbert)               | AIA_193_full_image_sonified.mid.mp3    |
| V A   | AIA 193 Å | Subimage 1 (Arcs)                      | subimage_1_x_685_y_1755.mid.mp3        |
| V A   | AIA 193 Å | Subimage 2 (Fan)                       | subimage_2_x_1060_y_1120.mid.mp3       |
| V A   | AIA 193 Å | Subimage 3 (Island)                    | subimage_3_x_1290_y_1690.mid.mp3       |
| V A   | AIA 193 Å | Subimage 4 (Limb)                      | subimage_4_x_1800_y_992.mid.mp3        |
| V A   | AIA 193 Å | Subimage 5 (Spot)                      | subimage_5_x_890_y_1035.mid.mp3        |
| V A   | AIA 193 Å | Subimage 6 (Swirl)                     | subimage_6_x_750_y_1125.mid.mp3        |
| V A   | AIA 193 Å | Subimage 7 (X)                         | subimage_7_x_760_y_405.mid.mp3         |
| V B   | AIA 193 Å | Filament liftoff montage               | liftoff_complete.mid.mp3               |

160 index of solar activity. It has been measured or derived for roughly 400 years. It is the source of  
 161 much of our knowledge of the evolution of solar activity. We use Version 2 of the International  
 162 Sunspot Number<sup>14,15</sup> between 01 Jan 1750 and 31 Dec 2018 from the Solar Influences Data analysis  
 163 Center (SIDC) website, both the monthly and annually averaged values. The time dependence of  
 164  $S$  is shown in Figure 1.

165 After some experimentation, we determined the following sonification. The annually-averaged  
 166 values were mapped to pitches between 48 and 96 of the lower timbre (PICKED\_BASS) and a  
 167 loudness of 125. This data was used to set the tempo (one year is one beat with a duration of a  
 168 quarter note) of 400 bpm. The monthly-averaged values were mapped to pitches between 60 and  
 169 108 in the PIANO timbre and a loudness of 100. This data is played at 12 values per beat (a group  
 170 of 12 thirty-second-note triplets), and was panned left-right with a two-year period. This allows  
 171 you to hear the differences in the two signals. The slower lower voice can be audibly distinguished  
 172 from the more rapidly varying higher voice.

173 You can listen to this sonification at

174 [https://sdo.gsfc.nasa.gov/iposter/mp3/TS\\_sunspot\\_annual\\_month.mid.mp3](https://sdo.gsfc.nasa.gov/iposter/mp3/TS_sunspot_annual_month.mid.mp3)



175

176 FIG. 1. Version 2 of the International Sunspot Number as a function of time since 1750. The solid blue line  
 177 is the annually-averaged data (plotted at the middle of each year) and the '+' symbols show the monthly-  
 178 averaged values.

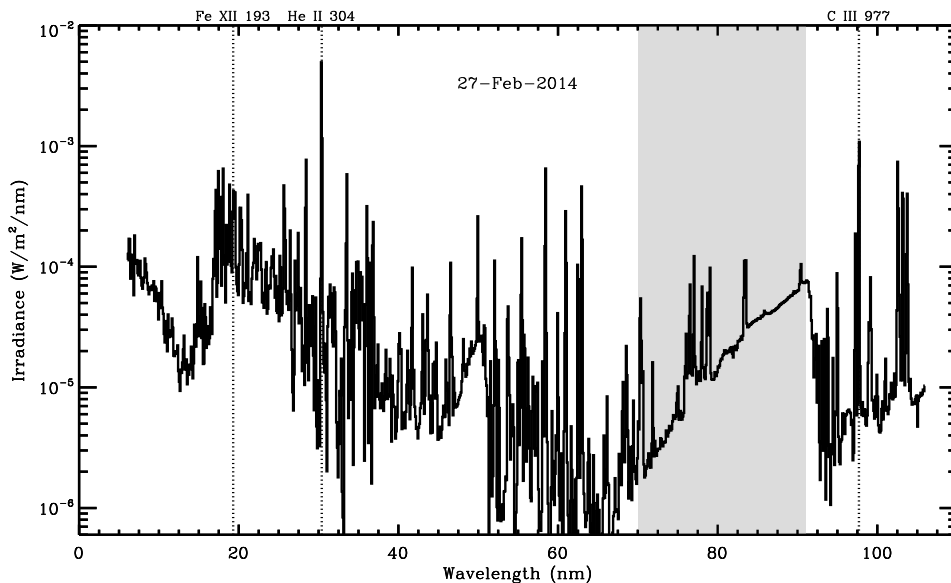
## 179 B. Extreme Ultraviolet Spectral Irradiances

180 The next example is to sonify extreme ultraviolet (EUV) spectral irradiances from two instru-  
 181 ments in two ways. The solar EUV spectral irradiance spans wavelengths between X-rays and  
 182 the ultraviolet (roughly 10–100 nm) but is often extended to include the H I 1216 emission line  
 183 (Ly- $\alpha$ ). (Emission lines are described by the element symbol, the ion state of the element [where  
 184 H I is neutral hydrogen, H II is singly-ionized hydrogen, etc.], and the wavelength of the line in  
 185 Å.) This radiation is easily absorbed as it ionizes the outer electrons of many elements. This also  
 186 makes it the major source of the ionosphere in the terrestrial and planetary atmospheres. The EUV  
 187 emissions are also a direct measure of the solar magnetic field. The Sun would have considerably  
 188 smaller EUV emissions if it did not have a magnetic field. For a 5770 K blackbody, the spectral ir-  
 189 radiance at an EUV wavelength of 30.4 nm is  $10^{-26}$  times the peak value at the visible wavelength  
 190 of 500 nm. This ratio is  $10^{-4}$  in an observed solar spectrum. These two properties, sensitivity to  
 191 the solar magnetic field and acting as the source of the ionosphere, make measurements of the solar  
 192 EUV spectral irradiance a primary goal in solar physics.



193 Solar EUV spectral irradiances are completely absorbed by the atmosphere and must be mea-  
 194 sured by an instrument in space. These instruments record the spectral irradiances as a function  
 195 of wavelength and time. We first sonify a single spectrum from the Extreme ultraviolet Variabil-  
 196 ity Experiment (EVE)<sup>16</sup> on NASA's Solar Dynamics Observatory (SDO).<sup>17</sup> EVE data is available  
 197 from 5 to 105 nm from 1 May 2010 until 26 May 2014 and from 37–105 nm thereafter. Figure 2  
 198 shows that the EUV spectral irradiance has many emission lines. Two of the strongest (He I 304  
 199 and C III 977) are labeled, and several roughly triangular regions of continuum emission (such as  
 200 the one highlighted between 70 nm and 91 nm.) The third label points to the emission line Fe XII  
 201 193, which will be explored in later sections.

202 We elected to sonify the day-averaged solar EUV spectrum from EVE on 27 Feb 2014, the day  
 203 of maximum sunspot number for Solar Cycle 24 (Figure 2). The log of the spectral irradiances was



204

205 FIG. 2. A day-averaged EUV spectral irradiance for 27 Feb 2014, as measured by EVE, plotted against the  
 206 wavelength in nm. Three wavelengths are identified with vertical dashed lines. The He II 304 Å line is the  
 207 brightest in this wavelength range, with the C III 977 Å line the next brightest. The 70–90 nm continuum  
 208 emission region is highlighted. The Fe XII 193 emission line will be analyzed in images below. Although the  
 209 total radiant energy in this spectrum is  $4.7 \text{ mW m}^{-2}$ , about  $10^{-5}$  times the total solar irradiance of  $1361 \text{ W}$   
 210  $\text{m}^{-2}$ , it is responsible for much of the ionization in the thermospheres of the Earth, Venus, and Mars.

212

213 scaled to MIDI frequencies 36–96. That means every order of magnitude in the data spans about  
214 1.5 octaves. The PIANO timbre was used, each value occupies an 8<sup>th</sup> note, the tempo was set to  
215 600 bpm, and the loudness was set to 80.

216 This example shows how the independent variable, in this case wavelength, does not have to  
217 be time to sonify a data set. The independent variable must at least provide an ordering of the  
218 data set, in this case with a uniform spacing between the data points. This was judged to be the  
219 most musical example. Some of Bach’s Goldberg Variations (BWV 988) sound much like this  
220 sonification. Variation 24, at around the 33-minute mark as played by Glenn Gould in his 1981  
221 album of the same name, has several long chromatic runs that sound like the gradual rise of the  
222 EUV spectrum between 70–91 nm. The rapid increases in pitch of the strong spectral lines also  
223 add musical contrast to this piece.

224 You can listen to this sonification at  
225 [https://sdo.gsfc.nasa.gov/iposter/mp3/TS\\_EVE\\_sonified.mid.mp3](https://sdo.gsfc.nasa.gov/iposter/mp3/TS_EVE_sonified.mid.mp3)

226 Spectral irradiances at selected wavelengths can also be extracted from the measurements as  
227 a function of time. The source of another set of EUV spectral irradiances is the Solar Extreme  
228 ultraviolet Experiment (SEE)<sup>18</sup> on NASA’s Thermosphere Ionosphere Mesosphere Energetics and  
229 Dynamics (TIMED) spacecraft, which provides daily values of the irradiances between 0.5 and  
230 195 nm. The spectral irradiances from 9 Feb 2002 to 11 May 2019 of several strong emission  
231 lines (He I 304, Ly- $\alpha$ , C IV 1548, and Fe XVI 335), along with the 0.1–7 nm soft X-ray radiometer  
232 channel, were sonified. The time dependence of these channels is shown in Figure 3. Pitches  
233 between 24 and 108 were interpolated from the log of the irradiances using the maximum and  
234 minimum of each channel as the limits. This forces the channels to have the same pitch range.  
235 The timbres were PIANO, PICKED\_BASS, TROMBONE, FLUTE, and MARIMBA, respectively.  
236 Each value occupies an eighth note, the tempo was set to 640 bpm and the loudness was set to 100.

237 You can listen to this sonification at  
238 [https://sdo.gsfc.nasa.gov/iposter/mp3/TS\\_SEE\\_sonified.mid.mp3](https://sdo.gsfc.nasa.gov/iposter/mp3/TS_SEE_sonified.mid.mp3)

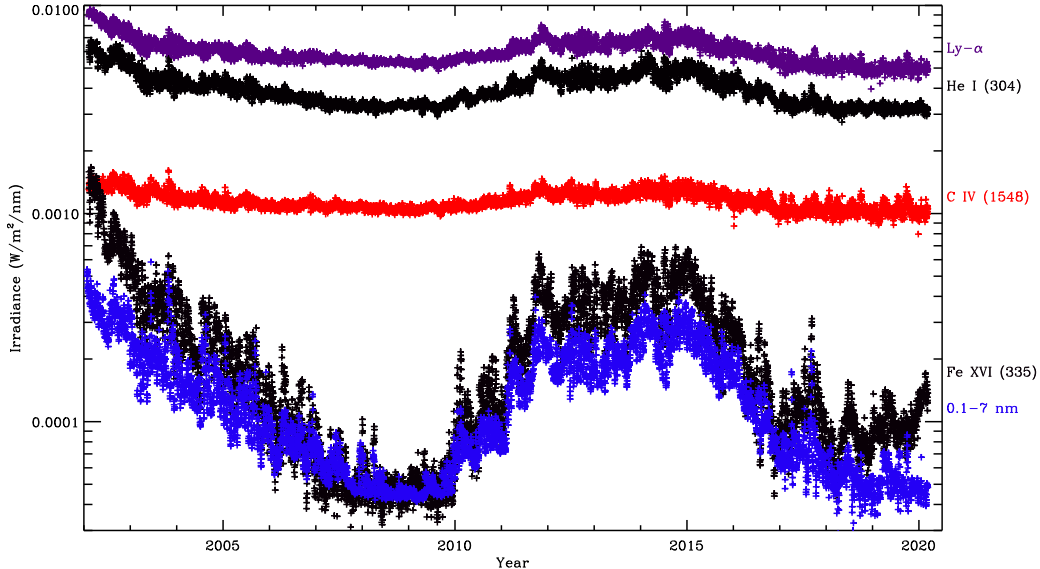


FIG. 3. The variation of selected EUV spectral irradiances from SEE with time. The selected wavelengths show different levels of solar cycle modulation. The Ly- $\alpha$  and 0.1–7 nm irradiances were divided by 10 and 20, respectively, before plotting.

### 239 C. Extreme Ultraviolet Images

240 Although measuring the EUV spectral irradiance is important, understanding those emissions  
 241 requires that you also have images at those wavelengths showing how the source regions of the  
 242 emissions vary in both space and time. Extreme ultraviolet images from the Atmospheric Imaging  
 243 Assembly (AIA)<sup>19</sup> on SDO were sonified as complete images, subimages, and a time sequence  
 244 of subimages. AIA provides 10 passbands: seven EUV, two ultraviolet, and one visible light.  
 245 AIA 193 Å images were selected as they highlighted the desired coronal details. We will describe  
 246 different ways to sonify an AIA 193 Å image from 23:55:53 UTC on 18 Mar 2018.

247 Compared with time series data, we found that images are difficult to sonify because they are  
 248 dense in information and have variations in two directions. As an example of density, a sonified  
 249  $512 \times 512$  image would take almost 15 hours to listen to at a moderate tempo of 300 bpm, and  
 250 a full-resolution ( $4096 \times 4096$ ) AIA image would require 40 days. Many people have a hard time  
 251 remembering tone sequences and whatever is happening near the end would be disconnected from  
 252 the beginning. We overcome this by either binning the image to a smaller number of pixels or

253 selecting subimages. Based on our experiences when playing our sonifications, where we found  
 254 that a person can remember tone sequences for a few minutes, we aim to create sonifications that  
 255 last three minutes by binning the image to  $32 \times 32$  pixels or by using much higher tempos (up  
 256 to 3000 bpm). Pieces such as John Cage’s *Organ<sup>2</sup>/ASLSP (As Slow as Possible)* may be written  
 257 for performance times of hours to years, but the density of notes is far smaller in these pieces.  
 258 Only 31 notes have been sounded since a 639 year version of the piece was begun in 2001 at the  
 259 Burchardikirche in Halberstadt, Germany.<sup>20</sup> One of our sonifications would sound 31 notes in the  
 260 first 6.2 s at our standard tempo of 300 bpm.

261 AIA science data is served as monochromatic,  $4k \times 4k$ , 14-bit files using the Flexible Image  
 262 Transport System (FITS).<sup>21</sup> To make these sonifications more accessible to students, we elected  
 263 to use the quicklook AIA images that are served as JPEG files created from the FITS data by  
 264 binning to a lower resolution (typically  $2048 \times 2048$  pixels), then applying a log scaling and an  
 265 arbitrary color table. Concentrating on converting JPEG images allowed us to test the algorithms  
 266 using images with higher contrast or more distinct features. This allows the students to sonify  
 267 their favorite images. When necessary the JPEG images were converted to greyscale using the  
 268 luminosity form of relative luminance to weight the individual red ( $R$ ), green ( $G$ ), and blue ( $B$ )  
 269 channels:

$$IM(B\&W) = 0.21R + 0.72G + 0.07B. \quad (1)$$

270 Although the solar images used have redundant information in the separate color channels, by  
 271 applying the luminosity form to all JPEG images it is possible to analyze any image with a three-  
 272 color format.

#### 273 **D. Raster-scan Sampling**

274 The greyscale images must now be converted into a 1-D series for sonification. The first ex-  
 275 ample is to sample them along a raster scan as described above. One initial image, binned from  
 276 dimensions of  $2048 \times 2048$  to  $32 \times 32$ , is shown in Figure 4, with the image overdrawn by the  
 277 raster scan used to generate the sampling curve in the lower plot. This image is also shown in  
 278 higher resolution and with fewer obscuring lines in Figure 7.

279 The pixels from the  $32 \times 32$  binned image were scaled by mapping values between  $[0, 250]$  to

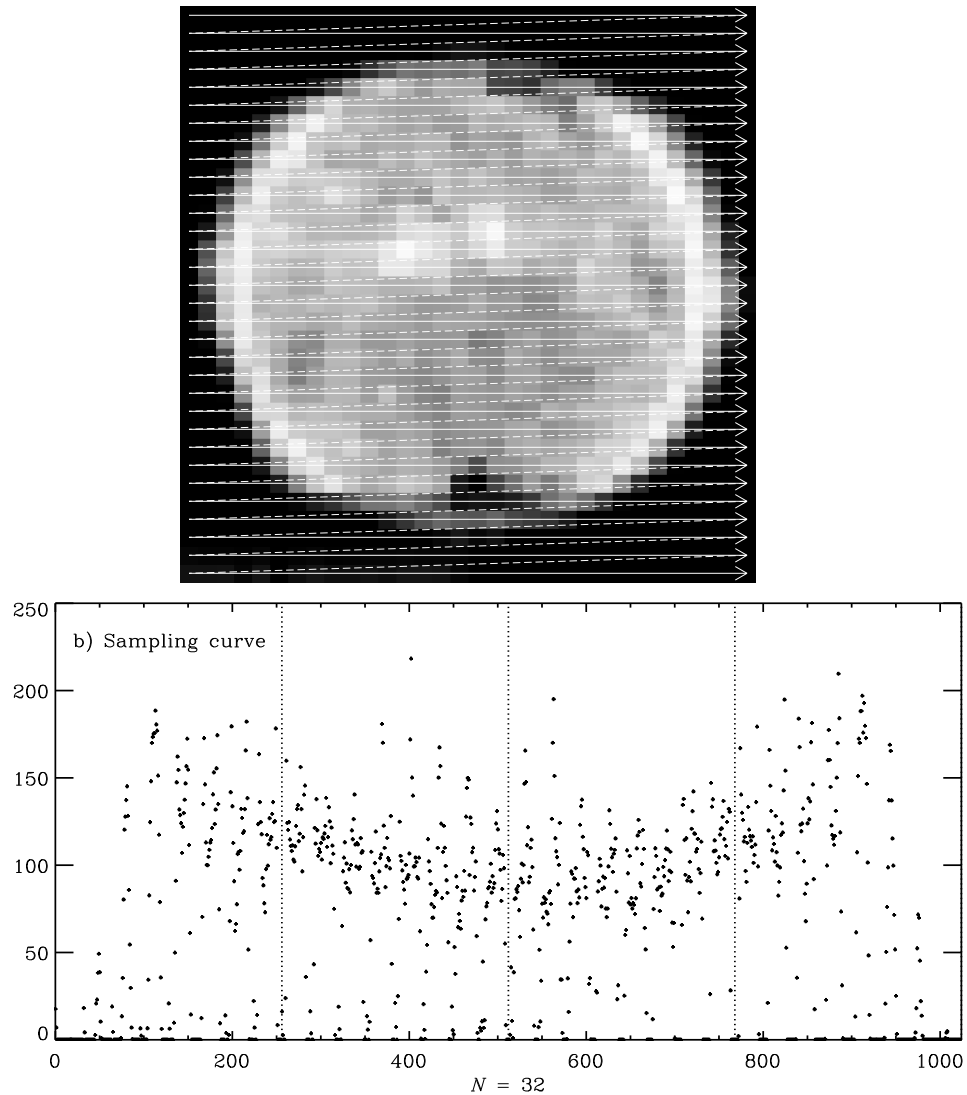


FIG. 4. A greyscale SDO/AIA 193 Å image from 18 Mar 2019 binned from  $2048 \times 2048$  to  $32 \times 32$ . At the top is an example of how a raster scan from the top left to the lower right samples the image. The dashed lines are the return from right to left that is not used in the sampling. The resulting sampling curve for this image is shown in the lower plot (b). The vertical lines show the four horizontal strips of the image.

280 pitches between [60, 120] (or C4 to C9, a span of 5 octaves). The duration was set to a sixteenth  
 281 note, the loudness to 110, and the SOPRANO\_SAX timbre was used.

282 You can listen to this sonification at

283 [https://sdo.gsfc.nasa.gov/iposter/mp3/AIA\\_193\\_full\\_image\\_sonified\\_raster.mp3](https://sdo.gsfc.nasa.gov/iposter/mp3/AIA_193_full_image_sonified_raster.mp3)

284 The lower curve (b) in Figure 4 shows how the raster scan is dominated by the quasi-periodic

285 variations caused by the scan moving onto and off of the disk of the Sun. We reduced some of the  
 286 noisy variations at low pixel values by replacing the dark regions with a rest, but the sonification  
 287 still does not reveal much about the image other than the broad shape of the Sun.

288 **One experiment was performed see if the sonification could be improved. Similar to the**  
 289 **sunspot series in § III A, a lower-resolution version of the series was sonified along with the**  
 290 **original. The image was sampled to a lower resolution using  $2 \times 2$  binning. Because of how**  
 291 **the raster scan addresses the pixels, the lower-resolution sampling is not the average value of**  
 292 **four successive values in the higher-resolution sampling, but it is the average of values in the**  
 293 **same region of the image. The relative timing of the voices is arbitrary, but the two sequences**  
 294 **were synchronized by using a duration ratio of four to one by sonifying the lower-resolution**  
 295 **image with quarter notes. However, we judged that the lower-resolution image tended to**  
 296 **only reinforce the quasi-periodic variations without providing useful additional information.**  
 297 **This experiment was not included in the published sonifications.**

298 Due to the poor results using a raster scan to sonify an image, we explored using other methods  
 299 to sample the image. The Hilbert curve was one of those methods.

#### 300 IV. HILBERT CURVES

301 Hilbert curves are continuous space-filling curves that have been used in a surprisingly large  
 302 number of disciplines. They were first described by Hilbert<sup>22</sup> as a simpler form of the space-filling  
 303 curves of Peano<sup>23</sup>. A true Hilbert curve exists only as the limit of  $n \rightarrow \infty$  of the  $n^{\text{th}}$  approximation  
 304 to a Hilbert curve ( $H_n$ ). However, the approximations are useful to provide mappings of 2-D  
 305 images onto a 1-D sequence. Figure 5 shows  $H_n$  for  $n = 1, 2, \dots, 6$ .

306 A summary of the properties of  $H_n$ :

- 307 1. There are  $2^n$  pixels along each side of the square containing the curve
- 308 2. The Euclidean length of  $H_n$  grows exponentially with  $n$ ,  $2^n - 2^{-n}$
- 309 3.  $H_n$  covers a finite area as it is always bounded by the unit square
- 310 4. Two points in the image,  $(x_1, y_1)$  and  $(x_2, y_2)$ , that are close together in  $H_n$  are also, with a  
 311 few exceptions, close together in  $H_{n'}$ ,  $n' > n$

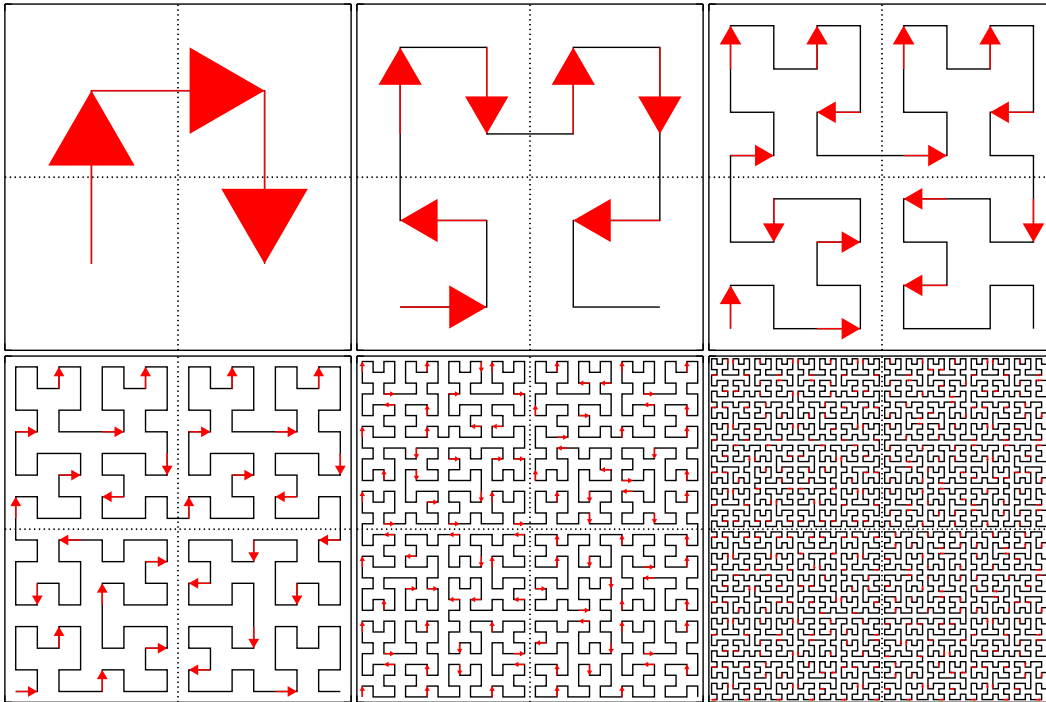


FIG. 5. The first six Hilbert curves, plotted from upper left to lower right, with arrows showing the direction of the motion into each vertex. Each subplot is drawn with axes limits of  $[0,1]$  in both directions. Among the most important properties of these curves is the single line connecting two quadrants. This can be seen by examining the dotted lines drawn to separate the quadrants. Another property is that the sampling goes around each quadrant in a similar motion (upper quadrants are sampled in a clockwise fashion and the lower quadrants in a counter-clockwise fashion.)

312 A Hilbert curve maps a linear variable onto the two-dimensional coordinates of an image. Its  
 313 inverse is a mapping of the image coordinates onto a linear variable. This mapping property means  
 314 we can use Hilbert curves to map solar images onto a linear sequence of pixel values that can then  
 315 be sonified. Images tend to have dimensions that are powers of 2, so the Hilbert curves are a natural  
 316 fit to addressing them.

317 Reading the image along a Hilbert curve has the advantage of keeping neighborhoods close to-  
 318 gether as the resolution (i.e., the length of the curve) increases. It also removes most of the detector  
 319 size periodicities and actually shows the presence of larger-scale features. **This locality property**  
 320 **means that averages to produce a slower-varying voice are well defined when an image is**  
 321 **sampled along a Hilbert curve. Let's assume you produce a sampling curve by addressing an**

322 **image with  $H_n$  and then reduce that curve by bin-averaging four points at a time. That new**  
 323 **curve has the same values that are found by averaging the image in  $2 \times 2$  subimages and then**  
 324 **sampling the lower-resolution image with  $H_{n-1}$ . Sampling curves at all resolutions can be**  
 325 **derived by recursively bin-averaging the next higher-resolution sampling curve four points**  
 326 **at a time. Even though averaging is not a musical operation, this equivalence is superior to**  
 327 **using a raster scan where bin-averaging the sampling curve and sampling a binned image do**  
 328 **not return the same value.**

329 The neighborhood property works with other space-filling curves. Bartholdi et al.<sup>24</sup> describe  
 330 using a Sierpinski space-filling curve to design delivery routes for Meals on Wheels. The system  
 331 was simple, cheap, and paper-based. It used a manual “Rolodex” method of entering or removing  
 332 addresses.

333 Vinoy et al.<sup>25</sup> and others have shown how to use Hilbert curves to construct microwave anten-  
 334 nas. They describe models and measurements of the input impedance to show that a small square  
 335 overlain with a conducting Hilbert curve produced an antenna whose resonance frequencies were  
 336 consistent with a much longer wire antenna. They also showed how those frequencies shifted and  
 337 how additional resonances were added as the order of the Hilbert curve was increased. This makes  
 338 these antennas useful for mobile wireless devices.

339 Seeger and Widmayer<sup>26</sup> describe using space-filling curves to access multi-dimensional datasets  
 340 with a 1-D addressing scheme. The 1-D curve imposes an order on the data access that is difficult  
 341 to implement using a multi-dimensional access polynomial. Morton<sup>27</sup> describes using the space-  
 342 filling Z-order curves to access a file address database. Like the Hilbert curve, Z-order curves  
 343 preserve the locality of most of the points being mapped.

344 Multi-dimensional Fourier integrals (as well as others) can be reduced to a 1-D form by map-  
 345 ping the coordinates onto a space-filling curve, essentially converting the integral into a Lebesgue  
 346 integral.<sup>28</sup>

## 347 V. EXTREME ULTRAVIOLET IMAGES SAMPLED ALONG HILBERT CURVES

348 A  $32 \times 32$  image can also be sampled using an  $n = 5$  Hilbert curve. This is shown in the top  
 349 panel of Figure 6. Similar to the raster scan method in § III D and the sunspot series in § III A, the



350 image was sampled in two different resolutions that are then played together. The higher register  
 351 was scaled from the  $32 \times 32$  binned image by mapping the pixel values between [0,250] to pitches  
 352 between [60, 120] (or C4 to C9, a span of 5 octaves). The duration was set to a sixteenth note,  
 353 the loudness to 110, and the SOPRANO\_SAX timbre was used. The lower register was added by  
 354 mapping pixels from a  $16 \times 16$  binned image with values between [0,250] to pitches [48, 96] (or  
 355 C3 to C7, a span of 4 octaves). The duration was set to a quarter note, the loudness to 90, and the  
 356 ACOUSTIC\_GRAND timbre was used. The lower register is the average value of the four pitches  
 357 in the higher register in the same region of the image and the two registers are synchronized.

358 You can listen to this sonification at  
 359 [https://sdo.gsfc.nasa.gov/iposter/mp3/whole\\_AIA\\_193\\_full\\_image\\_sonified.mid.mp3](https://sdo.gsfc.nasa.gov/iposter/mp3/whole_AIA_193_full_image_sonified.mid.mp3)

360 The difference between the sampling along a Hilbert curve and a raster scan can be seen by  
 361 comparing the lower curves in Figure 6 and Figure 4. The lower curve in Figure 6 shows the  
 362 Hilbert curve sampling localizes the off-disk portions of the image along the curve and hence in  
 363 time in the sonified version, while the lower curve in Figure 4 shows the raster scan has strong  
 364 modulations of the signal by the shape of the Sun.

### 365 A. Using Subimages to Emphasize Features in Extreme Ultraviolet Images

366 The AIA 193 Å image in Figure 6 is vastly undersampled. The number of pixels in a sonified  
 367 image scales as  $2^{2n}$ , where  $n$  is the order of the Hilbert curve used to sample the image. One way  
 368 to increase the accuracy of the sampling while keeping a reasonable length in the sonification is  
 369 to sub-sample the image. Seven  $64 \times 64$  subimages of the  $2048 \times 2048$  2019 Mar 18 image are  
 370 shown in Figure 7, numbered to agree with Table I.

372 Each subimage was sonified by being sampled along a Hilbert curve. The pixels in a  $64 \times 64$   
 373 patch were first binned to  $32 \times 32$  and then sampled with an  $n = 5$  Hilbert curve. The tones  
 374 were produced by mapping pixel values between [0, 255] to pitches between [60, 120] (or C4 to  
 375 C9). The duration was set to a sixteenth note, the tempo to 300 bpm, the loudness to 110, and  
 376 the SOPRANO\_SAX timbre was used. A second voice was added by mapping the pixels from a  
 377  $16 \times 16$  binned image with values between [0,255] to pitches [48, 84] (or C3 to C6, a span of 3  
 378 octaves). The duration was set to a quarter note, the loudness to 75, and the ACOUSTIC\_GRAND

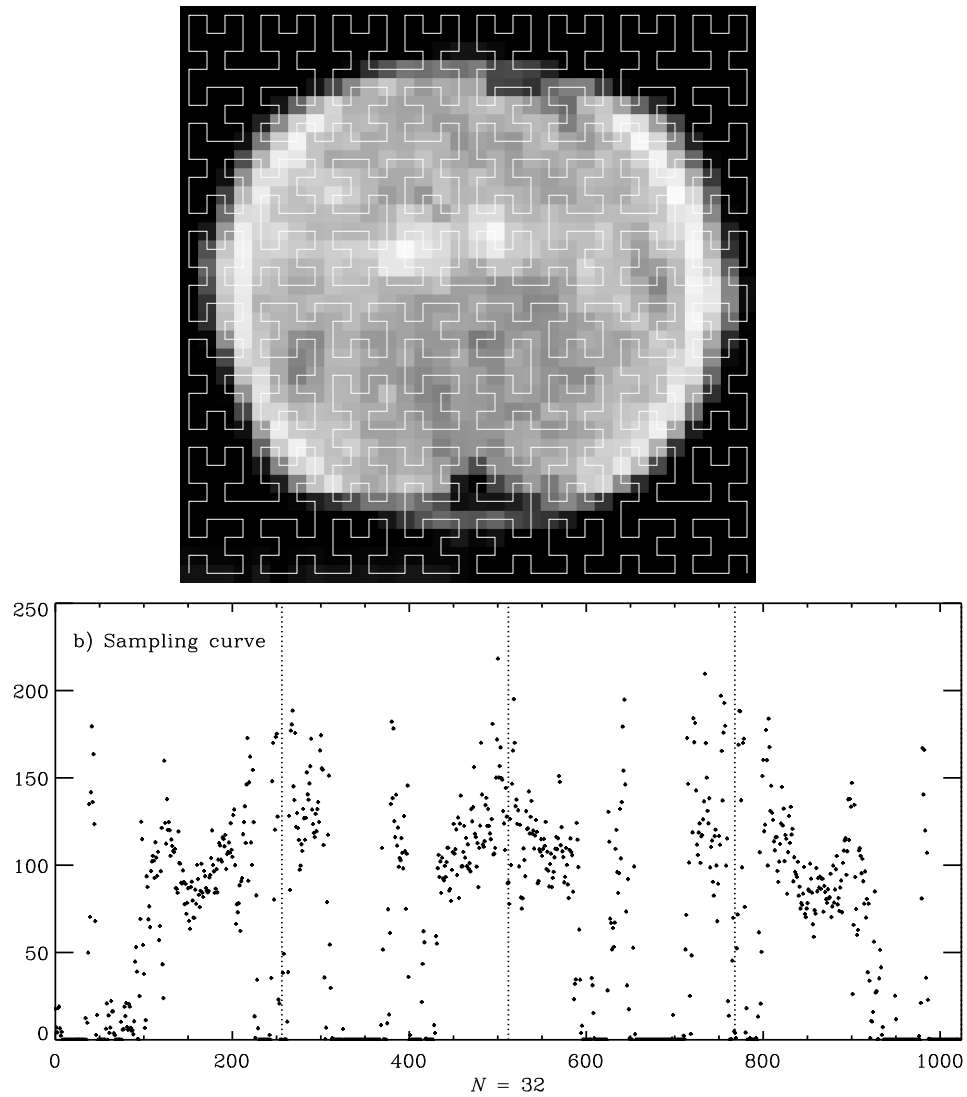


FIG. 6. The top panel has an  $n = 5$  Hilbert curve ( $H_5$ ) drawn over the greyscale SDO/AIA 193 Å image from 18 Mar 2019 binned from  $2048 \times 2048$  to  $32 \times 32$ . The lower plot (b) shows the resulting sampling curve. Each pixel in the image is assigned to a point in the curve. The centers of square pixels are located where the curve has a right angle bend, at the halfway mark of straight segments that are two units long, or two centers proportionally spaced along the straight segments that are three units long. The vertical lines show the four quadrants of the image.

379 timbre was used.

380 You can listen to this sonifications by accessing the clickable image at

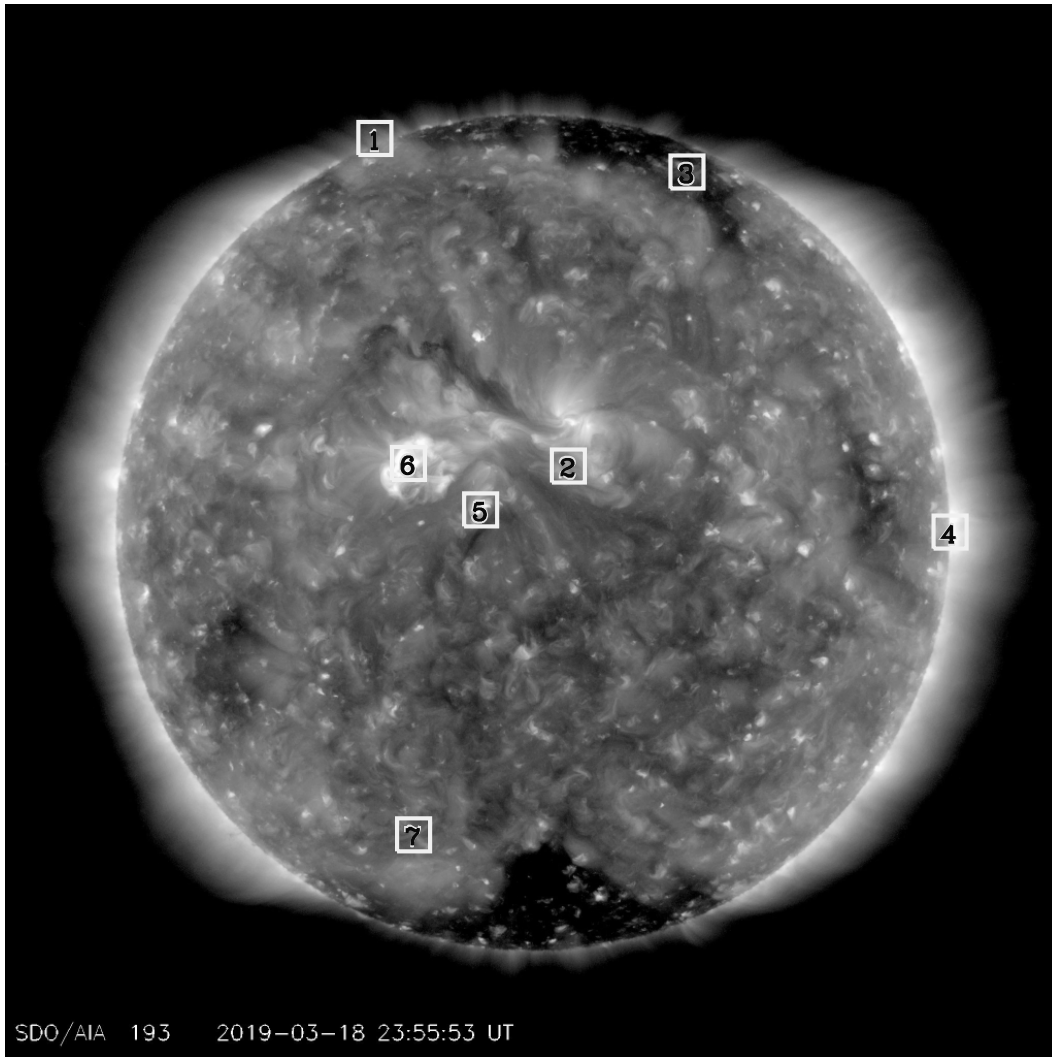


FIG. 7. A greyscale SDO/AIA 193 Å image from 18 Mar 2019. This image was used as an example for sonifying still images in § III D and § V. The boxes mark the locations of the examples in Table I.

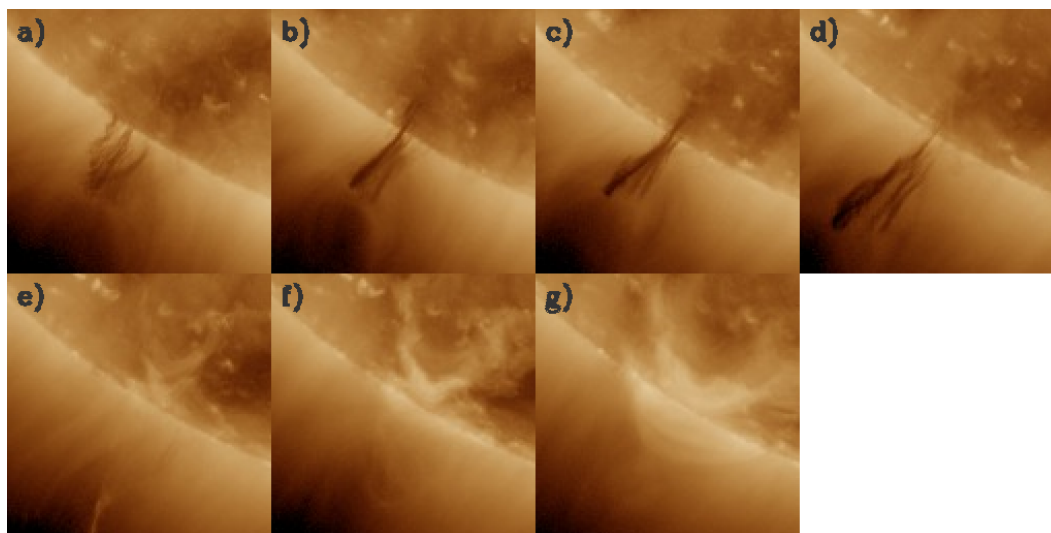
381 <https://sdo.gsfc.nasa.gov/iposter/>.

### 382 **B. Filament Liftoff Sequence in Extreme Ultraviolet Images**

383 The final example is sonifying a series of  $2048 \times 2048$  images from AIA on SDO. The goal  
 384 is to determine whether the time sequence in the images can be heard. We selected the filament  
 385 liftoff of 10–12 Mar 2010 as an example (Figure 8). Eight  $128 \times 128$  subimages that included  
 386 the filament liftoff were extracted, binned to  $32 \times 32$ , sampled along an  $n = 5$  Hilbert curve and

387 sonified. A short chorus and ending cadence were written. The piece was made by inserting the  
 388 subimages in turn, separated by a chorus and ending with the cadence, thus creating a single time  
 389 series of pitches.

390 The early results for this sequence were not very successful. We then tried several ways to  
 391 improve the sonification. First, the length of the individual frames was reduced by including only  
 392 the lower-left and upper-left quadrants of those subimages. This corresponds to the first half of the  
 393 sequence sampled by the Hilbert curve. When this did not produce a satisfactory result, we selected  
 394 only those images with a noticeable difference. This produced seven images that emphasized the  
 395 variation but were unevenly spaced in time. Finally, the pixels in this sequence were converted  
 396 to tones by subtracting the average of each image from the sampled data, mapping the resulting  
 397 values from  $[-60, 60]$  to pitches  $[36, 96]$  (or C2 to C7, a span of 5 octaves). The duration was set  
 398 to a sixteenth note, the loudness to 110, and the PIANO timbre was used. Only the final attempt  
 399 that includes all of these steps is presented here.



400

401 FIG. 8. Montage of the final seven solar images showing a filament liftoff. Starting from the upper left,  
 402 the images were recorded at a) 2012-03-10 02:27:20, b) 2012-03-11 03:27:44, c) 2012-03-11 17:59:08, d)  
 403 2012-03-11 23:29:08, e) 2012-03-12 01:29:20, f) 2012-03-12 02:28:56, g) 2012-03-12 04:27:56, and h)  
 404 2012-03-12 06:29:56, respectively. (All times are UTC).

405 You can listen to this sonification at

406 [https://sdo.gsfc.nasa.gov/iposter/mp3/liftoff\\_complete.mid.mp3](https://sdo.gsfc.nasa.gov/iposter/mp3/liftoff_complete.mid.mp3)

407 This was the least satisfying sonification because the changes in time were subtle and difficult  
408 to resolve. We have been investigating other ways to show the movement of material through  
409 both space and time. The subtraction of the mean was one example of one such a technique.  
410 By removing the average any overall brightening or darkening of the region did not dominate the  
411 change in time. Another possibility is to sonify the running difference images that AIA produces.  
412 We have sonified shapes moving through space to study this effect. Part of the issue is the large  
413 number of redundant pixels that do not significantly change value in time. Sonifying a sequence in  
414 time remains an area of active research.

## 415 VI. DISCUSSION OF SONIFIED DATA

416 Based on our experiments, percussive sounds, such as PIANO and PICKED\_BASS, seem to  
417 work better for sonifying data. Percussive timbres securely place the sound on the beat and produce  
418 interesting changes as the tempo increases. A timbre with a noticeable rise or decay time tends to  
419 sound muddy as the tempo is increased.

420 Our attempts to create a beat and melody by playing two versions of averaged data, such as the  
421 annual vs. the monthly values of  $S$ , were not a complete success. We continue to explore how to  
422 make the sonified data sound more like music and less mechanical.

423 Although sonified data does not sound like most types of music, at least some pieces of classical  
424 music has similar qualities. Bach's Goldberg Variations (BWV 988) sounds much like the image  
425 sonifications described above. As we note above, the chromatic runs in Variation 24, at around  
426 the 33-minute mark as played by Glenn Gould in his 1981 album of the same name, sound quite  
427 similar to the EVE spectrum.

428 Sonifying data streams is a flexible area of study. To skip the image analysis step, you can load  
429 the MIDI files provided for each of the sonifications into any compatible synthesizer. This will  
430 immediately reveal that different synthesizers assign different timbres to each numbered track, so  
431 the files will sound different in each synthesizer. You can also change the timbre of a part in  
432 the synthesizer, providing another level of experimentation. Other sound font files can also be  
433 used with the synthesizers, including the JythonMusic synthesizer, again providing another area to  
434 explore.

435 This also explains why the provided MP3 files do not always match what was heard when the  
436 JythonMusic synthesizer is used. You cannot create an MP3 file directly from the JythonMusic  
437 synthesizer. You can capture the sounds in either a recorder or software such as Audacity while  
438 the MIDI commands are executed. Or you can load the file containing the commands into another  
439 synthesizer that has export capability. The MP3 files provided here were created by opening the  
440 MIDI files in GarageBand, a proprietary program from Apple, and exporting the MP3 files.

441 You can also use other programs to generate the MIDI file from a dataset. For example,  
442 Lilypond<sup>29</sup> is a music engraving program that can also produce a MIDI file that is playable in a  
443 MIDI-capable synthesizer. You also get a beautiful score of the piece as a bonus. Similar to the  
444 JythonMusic workflow, the data file was opened in Python, the data was scaled to pitches and those  
445 pitches were written in Lilypond syntax to a Lilypond-readable text file. An example of a score is  
446 shown in Figure 9. Strong spectral lines can be seen in measures 31 and 35.

448 Mapping data to variations in pitch may not be the optimum solution for sonifying data. A large  
449 value of a dataset may be better represented by changes in the volume, emphasizing the strength of  
450 the larger value. We did some experiments on such variations and found that the limited ability of  
451 humans to sense changes in loudness and to remember a baseline level of loudness over an entire  
452 piece made this less effective at sonifying data. Sonifying the data using a constant pitch with  
453 variable loudness also led to annoyance caused by the unchanging pitch.

454 Following on the success of whistlers, numerous other datasets from solar physics and related  
455 fields of research were sonified, such as the variations of the solar wind.<sup>30,31</sup> Solar sound waves  
456 propagating in the resonant chamber of the solar interior are observed as wave fields at the solar  
457 surface. The size of and run of temperature inside the Sun mean these waves have frequencies of  
458 several mHz, which can be inverted to probe the solar interior.<sup>32</sup> The waves have been audified  
459 by frequency shifting them to audible ranges.<sup>6,7</sup> Those examples are for 1-D time series. In an-  
460 other the motion of a person is used to sample an image and create an interactive image-to-music  
461 experience.<sup>33</sup> Others have produced a sonified solar system.<sup>34</sup> The image sonifications described  
462 herein may be one of the few examples of such a project.

**EUV on 27 Feb 2014 (Solar Maximum)**

Piano Old Sol

FIG. 9. The first page of a piano score of the EVE spectrum in Figure 2 created by Lilypond. The He II 304 Å line can be seen in measure 31 and the Fe XVI 335 Å line in measure 35. The scaling to pitch is different than the sonified example to better fit on the staves.

## 463 VII. CONCLUSIONS

464 We have sonified a sunspot time series, an EUV spectrum, a time series of EUV spectral irradi-  
 465 diances, EUV images with various techniques, and a time sequence of EUV images. The EUV  
 466 spectrum showed that the independent variable does not have to be time. We demonstrated that  
 467 using a Hilbert curve to address a solar image gives a sonification that shows more of the image  
 468 variations and less of the shape of the Sun. **The locality property of the Hilbert curve ensures**  
 469 **the method of using multi-resolution sampling curves to sonify the image in different voices**  
 470 **is a well-defined operation that produces synchronized voices.**

471 **The commutability of the binning operators in the Hilbert sampling method could have**  
 472 **other ramifications in image analysis. Any operation on the image, such as compression, that**

473 **employs smoothing could offer superior results using a Hilbert curve sampling.**

474 One shortcoming of the Hilbert curve sampling method is the separation of two regions near the  
475 limb. In these examples, images are sampled by a curve that crosses from the upper left quadrant  
476 to the upper right near the equator. This means the northern polar region is sampled in two distinct  
477 areas far from one another. The two lower quadrants do not have a direct connection, so the  
478 southern polar region is also divided into two distinct regions, one at the beginning of the series  
479 and the other at the end. This can be remedied by rotating the Hilbert curve (or the image) 90°  
480 in either direction, which moves the connection between quadrants to the poles and keeps those  
481 regions in a smaller neighborhood while dividing the equatorial limb sectors into disparate parts of  
482 the sampling curve.

483 Other techniques can be used to sonify solar images. Coincident images observed in different  
484 wavelengths of light can be sampled and placed in different timbres or pan positions. Once the next  
485 solar maximum passes, another EVE spectrum could be used to play against the solar maximum  
486 spectrum illustrated here. Higher-order Hilbert curves can be constructed to sample a series of  
487 images. This would keep points within a neighborhood in both space and time. Software that  
488 directly produces sounds rather than adhering to the MIDI standard might create sonifications that  
489 better represented the data. This could overcome the limited number of pitches available in the  
490 MIDI standard.

491 Sonifying solar images is a way to explore the interface between tempo and pitch. Increasing  
492 the tempo to 3000 bpm (or 50 Hz) allows you to investigate whether an extremely rapid tempo  
493 results in an envelope with the individual pitches providing an amplitude modulation of that enve-  
494 lope. Frequencies of 15–30 Hz (900–1800 bpm) are near the limit of pitch discrimination.<sup>35</sup> The  
495 difference between the buzz saw of the raster scan image (Sec. III D) and the smoother sound of  
496 Hilbert curve sampling of Sec. V is one example of how the envelope makes a big difference in the  
497 perception of the data.

498 Listening to the Sun allows people to enjoy our closest star in a new direction. This does not  
499 apply only to the blind, most people can hear the variations of the Sun. With time these techniques  
500 will also allow people to more fully explore images.



## 501 VIII. QUESTIONS AND OTHER PROJECTS

502 Many projects can come from data-driven sonifications. There are also many ways to do those  
503 sonifications. We selected the JythonMusic synthesizer because we could load any data we wanted  
504 into the program. Once the MIDI exists it can be loaded into any compatible synthesizer for play-  
505 back or experimenting.

506 Here are some suggestions that can motivate students to listen to their data:

- 507 1. A simple way to sonify an image is to put the sampled pixels into a sound file, such as a WAV  
508 file and played at the CD sample rate of 44100 samples per second. This “audification” of  
509 an image does not require a synthesizer. The file can be opened in most media players and  
510 listened to. Compare the audified image with the sonified image and describe the differences,  
511 aside from the speed of the audified image.
- 512 2. Can you find ways to vary the tempo of the music to represent variations in a data set?  
513 Scientific data tends to have even spacing and the simplest way to sonify the data is to  
514 maintain an even tempo. You can use the JythonMusic routine `Mod.tiePitches` to tie together  
515 identical notes to add some variety to the rhythmic spacing. Another routine, `Mod.accent`  
516 allows you to accent a beat, which also provides some rhythmic texture to the music.
- 517 3. Can loudness be used to emphasize important features in a log-scaled variable? Comparing  
518 the score of the spectrum in Figure 9 with the physical data in Figure 2, we can see that a  
519 few emission lines outshine much of that spectral region but that dominance is not reflected  
520 in the sonification. Perhaps increasing the loudness of the strong emission lines would better  
521 illustrate this dominance.
- 522 4. Three-color AIA images are created by putting coincident images in different wavelengths  
523 into individual color channels. These can be sonified by assigning a voice and pan position  
524 to each of the channels that will audibly emphasize the differences in the channels.
- 525 5. A wavelet analysis of a time series can be used to isolate persistent from ephemeral frequen-  
526 cies. Can a wavelet spectrum be sonified to show the persistent frequencies as droning notes  
527 and ephemeral events as more rapid variations?

528 6. Can other instruments be played against the synthesizer output? The sonified data has no  
 529 explicit key, so improvised solos and rhythms can be played along with the sonified data.

## 530 ACKNOWLEDGMENTS

531 Version 4.6 of the JythonMusic software was downloaded from <https://jythonmusic.me>. All of  
 532 the data used in this research is available as continually updated files from publicly-accessible sites.  
 533 The monthly averaged (SN\_m\_tot\_V2.0.csv) and the annually averaged (SN\_y\_tot\_V2.0.csv) In-  
 534 ternational Sunspot Number (Version 2) data were obtained from the Solar Influences Data Cen-  
 535 ter (<http://sidc.oma.be/silso/datafiles>). Daily averaged SEE measurements were obtained as  
 536 the SEE Level 3 Merged NetCDF file at [http://lasp.colorado.edu/data/timed\\_see/level3/latest\\_](http://lasp.colorado.edu/data/timed_see/level3/latest_see_L3_merged.ncdf)  
 537 [see\\_L3\\_merged.ncdf](http://lasp.colorado.edu/data/timed_see/level3/latest_see_L3_merged.ncdf). Daily averaged EVE measurements were obtained from the EVE Level 3  
 538 Merged NetCDF file at [http://lasp.colorado.edu/eve/data\\_access/evewebdataproducts/merged/](http://lasp.colorado.edu/eve/data_access/evewebdataproducts/merged/EVE_L3_merged_1a_2019135_006.ncdf)  
 539 [EVE\\_L3\\_merged\\_1a\\_2019135\\_006.ncdf](http://lasp.colorado.edu/eve/data_access/evewebdataproducts/merged/EVE_L3_merged_1a_2019135_006.ncdf). AIA images were obtained as JPEGs from the SDO  
 540 website <https://SDO.gsfc.nasa.gov>.

---

541 <sup>1</sup> Sabina Teller Ratner. *Camille Saint-Saëns, 1835-1921: A Thematic Catalogue of His Complete Works*,  
 542 volume 1. Oxford Univ. Press, New York, 2002. pp. 185–192.

543 <sup>2</sup> Dieter Daniels. Luigi russolo nintonarumoriz, 2020. URL [http://www.medienkunstnetz.de/works/](http://www.medienkunstnetz.de/works/intonarumori/audio/1/)  
 544 [intonarumori/audio/1/](http://www.medienkunstnetz.de/works/intonarumori/audio/1/).

545 <sup>3</sup> Iannis Xenakis. *Electro-Acoustic Music*. Vinyl LP, Nonesuch H-71246, 1970.

546 <sup>4</sup> Roger Luther. *Moog Archives*. URL <http://moogarchives.com>.

547 <sup>5</sup> Robert A. Helliwell. *Whistlers and Related Ionospheric Phenomena*. Dover Publications, Inc., 2006.  
 548 Originally published by Stanford University Press, Stanford, California (1965).

549 <sup>6</sup> Alexander G. Kosovichev. *Solar Sounds*, 1997. URL <http://soi.stanford.edu/results/sounds.html>.

550 <sup>7</sup> Tim Larson. *SoSH Project: Sonification of Solar Harmonics*, 2020. URL [http://solar-center.stanford.](http://solar-center.stanford.edu/sosh/)  
 551 [edu/sosh/](http://solar-center.stanford.edu/sosh/).

- 552 <sup>8</sup> John H. Flowers. Thirteen years of reflection on auditory graphing: Promises, pitfalls, and potential new  
553 directions. In *Proceedings of ICAD 05-Eleventh Meeting of the International Conference on Auditory*  
554 *Display, Limerick, Ireland, July 6-9, 2005*, pages 406–409, 2005.
- 555 <sup>9</sup> The MIDI Association. Midi association, 2020. URL <https://www.midi.org>.
- 556 <sup>10</sup> Bill Manaris and Andrew R. Brown. *Making Music with Computers: Creative Programming in Python*.  
557 Taylor and Francis Group, LLC, Boca Raton, Florida, 2014.
- 558 <sup>11</sup> John Backus. *The Acoustical Foundations of Music*. W. W. Norton & Company, New York, 1969. p.  
559 113.
- 560 <sup>12</sup> Frederik Temmermans. JPEG, 2020. URL <https://jpeg.org/index.html>.
- 561 <sup>13</sup> John Backus. *The Acoustical Foundations of Music*. W. W. Norton & Company, New York, 1969. The  
562 Fletcher-Munson curves in this work have been revised and updated in ISO 226:2003 but the conclusions  
563 needed here remain valid.
- 564 <sup>14</sup> F. Clette, L. Svalgaard, J. M. Vaquero, and E. W. Cliver. Revisiting the Sunspot Number. A 400-Year  
565 Perspective on the Solar Cycle. *Space Sci. Rev.*, 186:35–103, December 2014. doi:10.1007/s11214-014-  
566 0074-2.
- 567 <sup>15</sup> Frédéric Clette and Laure Lefèvre. The new sunspot number: Assembling all corrections. *Solar Phys.*,  
568 291:2629–2651, 2016. doi:10.1007/s11207-016-1014-y.
- 569 <sup>16</sup> T. N. Woods, F. G. Eparvier, R. Hock, A. R. Jones, D. Woodraska, D. Judge, L. Didkovsky, J. Lean,  
570 J. Mariska, H. Warren, D. McMullin, P. Chamberlin, G. Berthiaume, S. Bailey, T. Fuller-Rowell, J. Sojka,  
571 W. K. Tobiska, and R. Viereck. Extreme Ultraviolet Variability Experiment (EVE) on the Solar Dynamics  
572 Observatory (SDO): Overview of Science Objectives, Instrument Design, Data Products, and Model  
573 Developments. *Solar Phys.*, 275:115–143, January 2012. doi:10.1007/s11207-009-9487-6.
- 574 <sup>17</sup> W. D. Pesnell, B. J. Thompson, and P. C. Chamberlin. The Solar Dynamics Observatory (SDO). *Solar*  
575 *Phys.*, 275:3–15, January 2012. doi:10.1007/s11207-011-9841-3.
- 576 <sup>18</sup> T. Woods, S. Bailey, F. Eparvier, G. Lawrence, J. Lean, B. McClintock, R. Roble, G. Rottman,  
577 S. Solomon, and W. Tobiska. TIMED Solar EUV experiment. *Physics and Chemistry of the Earth*  
578 *C*, 25:393–396, 2000. doi:10.1016/S1464-1917(00)00040-4.
- 579 <sup>19</sup> J. R. Lemen, A. M. Title, D. J. Akin, P. F. Boerner, C. Chou, J. F. Drake, D. W. Duncan, C. G. Edwards,  
580 F. M. Friedlaender, G. F. Heyman, N. E. Hurlburt, N. L. Katz, G. D. Kushner, M. Levay, R. W. Lindgren,

- 581 D. P. Mathur, E. L. McFeaters, S. Mitchell, R. A. Rehse, C. J. Schrijver, L. A. Springer, R. A. Stern,  
582 T. D. Tarbell, J.-P. Wuelser, C. J. Wolfson, C. Yanari, J. A. Bookbinder, P. N. Cheimets, D. Caldwell,  
583 E. E. Deluca, R. Gates, L. Golub, S. Park, W. A. Podgorski, R. I. Bush, P. H. Scherrer, M. A. Gummin,  
584 P. Smith, G. Auken, P. Jerram, P. Pool, R. Soufli, D. L. Windt, S. Beardsley, M. Clapp, J. Lang, and  
585 N. Waltham. The Atmospheric Imaging Assembly (AIA) on the Solar Dynamics Observatory (SDO).  
586 *Solar Phys.*, 275:17–40, January 2012. doi:10.1007/s11207-011-9776-8.
- 587 <sup>20</sup> John-Cage-Orgel-Kunst-Projekt. Organ<sup>2</sup>/aslsp. URL <https://www.aslsp.org/de/klangwechsel.html>.
- 588 <sup>21</sup> W. D. Pence, L. Chiappetti, C. G. Page, R. A. Shaw, and E. Stobie. Definition of the Flexible Im-  
589 age Transport System (FITS), version 3.0. *A. & Ap.*, 524:A42, December 2010. doi:10.1051/0004-  
590 6361/201015362.
- 591 <sup>22</sup> D. Hilbert. Über die stetige abbildung einer linie auf ein flächenstück. *Mathematische Annalen*, 38:  
592 459–460, 1891.
- 593 <sup>23</sup> G. Peano. Sur une courbe, qui remplit toute une aire plane. *Mathematische Annalen*, 36:157–160, 1890.
- 594 <sup>24</sup> John J. Bartholdi, Loren K. Platzman, R. Lee Collins, and William H. Warden. A minimal technology  
595 routing system for Meals on Wheels. *Interfaces*, 13(3):1–8, 1983.
- 596 <sup>25</sup> K. J. Vinoy, K. A. Jose, V. K. Varadan, and V. V. Varadan. Hilbert curve fractal antenna: A small resonant  
597 antenna for VHF/UHF applications. *Microwave Opt Technol Lett*, 29(4):215–219, 2001.
- 598 <sup>26</sup> Bernhard Seeger and Peter Widmayer. Geographic information systems. In Sartaj Sahni and Dinesh P.  
599 Mehta, editors, *Handbook of Data Structures and Applications*, chapter 56. CRC Press, Boca Raton,  
600 Florida, 2nd edition, 2018.
- 601 <sup>27</sup> G. M. Morton. A computer oriented geodetic data base; and a new technique in file sequencing. Technical  
602 report, IBM Ltd., Ottawa, Canada, 1966.
- 603 <sup>28</sup> Norbert Wiener. *The Fourier Integral and Certain of its Applications*. Dover, New York, 1933.
- 604 <sup>29</sup> Lilypond. Lilypond . . . music notation for everyone, 2020. URL <http://lilypond.org>.
- 605 <sup>30</sup> Robert L. Alexander. Solar wind sonification, 2011. URL [http://www.srl.caltech.edu/ACE/](http://www.srl.caltech.edu/ACE/ACENews/ACENews144.html)  
606 [ACENews/ACENews144.html](http://www.srl.caltech.edu/ACE/ACENews/ACENews144.html).
- 607 <sup>31</sup> Andrea effe Rao. Sounds from the Sun - Data Sonification - Thesis, 2016. URL [https://www.behance.](https://www.behance.net/gallery/35831845/Sounds-from-the-Sun-Data-Sonification-Thesis)  
608 [net/gallery/35831845/Sounds-from-the-Sun-Data-Sonification-Thesis](https://www.behance.net/gallery/35831845/Sounds-from-the-Sun-Data-Sonification-Thesis).

- 609 <sup>32</sup> Michael J. Thompson. Helioseismology and the Sun's interior. *Astron. Geophys.*, 45(4):4.21–4.25, 08  
610 2004. doi:10.1046/j.1468-4004.2003.45421.x.
- 611 <sup>33</sup> Marty Quinn. “Walk on the Sun”: An interactive image sonification exhibit. *AI & SOCIETY*, 27(2):  
612 303–305, 2012. doi:10.1007/s00146-011-0355-1. URL <https://doi.org/10.1007/s00146-011-0355-1>.
- 613 <sup>34</sup> Michael Quinton, Iain McGregor, and David Benyon. Sonifying the solar system. In *The 22nd Interna-*  
614 *tional Conference on Auditory Display (ICAD-2016)*, pages 28–35, 07 2016. doi:10.21785/icad2016.003.
- 615 <sup>35</sup> John Backus. *The Acoustical Foundations of Music*. W. W. Norton & Company, New York, 1969. Ch. 7.